

## Observation of core electron temperature rise in response to an edge cooling in toroidal helical plasmas

N. Tamura, S. Inagaki, K. Ida, T. Shimozuma, S. Kubo, T. Tokuzawa, and K. Tanaka  
National Institute for Fusion Science, Toki, 509-5292, Japan

S. V. Neudatchin

Institute of Nuclear Fusion, Russian Research Center "Kurchatov Institute", Kurchatov square 1, Moscow 123182, Russia

K. Itoh, D. Kalinina, S. Sudo, Y. Nagayama, K. Ohkubo, K. Kawahata, A. Komori, and LHD Experimental Group

National Institute for Fusion Science, Toki, 509-5292, Japan

(Received 5 October 2005; accepted 10 October 2005; published online 22 November 2005)

The first observation of a significant rise of core electron temperature in response to edge cooling in a helical plasma has been made on the Large Helical Device [O. Motojima *et al.*, Phys. Plasmas **6**, 1843 (1999)]. When the phenomenon occurs, the electron heat diffusivity in the core region is reduced abruptly without changing local parameters in the region of interest. Therefore the phenomenon can be regarded as a so-called "nonlocal" electron temperature rise observed so far only in many tokamaks. © 2005 American Institute of Physics. [DOI: [10.1063/1.2131047](https://doi.org/10.1063/1.2131047)]

The clarification of electron heat transport in magnetically confined plasmas is still an important issue, since the performance of a probable fusion reactor should be determined by electron heating as a result of the interaction between electrons and alpha particles as a fusion reaction product. In order to promote a better understanding of the electron heat transport, the electron heat transport analysis for both transient and steady state has been carried out diligently in many tokamaks<sup>1-3</sup> and helical systems.<sup>4-6</sup> One of the significant issues found in these studies is a "nonlocal transport phenomenon" observed in perturbation experiments on many tokamaks<sup>7-12</sup> and a few helical systems.<sup>4</sup> In particular, a rise of the core electron temperature  $T_e$  invoked by the rapid cooling of the edge plasma has been observed in various tokamaks with both ohmically heated plasmas and plasmas with an auxiliary heating, such as electron cyclotron heating (ECH), at a sufficiently low density (e.g., Ref. 13). The amplitude reversal of the cold pulse propagation in the core plasma cannot be explained even by the model based on the assumption that heat flux has a strong nonlinear dependence on temperature and its gradient. In addition there seem to be no changes in the thermodynamic forces, such as those due to the temperature gradient and/or the density gradient, in the core plasma at the onset of the core  $T_e$  rise. Consequently, the core  $T_e$  rise invoked by the edge cooling is considered to result from a nonlocality in the electron heat transport. On the contrary, such a core  $T_e$  rise in response to the edge cooling has not been observed so far in helical systems.<sup>14</sup> Recently, to rationalize the so-called "nonlocal"  $T_e$  rise, some physics-based transport models including a critical gradient scale length, such as the ion temperature gradient (ITG) model, have been set up and tested.<sup>2,15</sup> It should be noted that despite being dependent on local variables, the ITG-based model shows a nonlocal response to small changes in the profiles as a result of a slight deviation from near marginality. The ITG-based model with strongest

stiffness<sup>16</sup> can reproduce some of the same qualitative characteristics observed in carbon laser blow-off experiments in the Texas Experimental Tokamak (TEXT).<sup>13</sup> The magnitude and response time of the core  $T_e$  rise, however, are still in quantitative disagreement with those predicted by the strongest stiff ITG-based model.<sup>15</sup> Moreover, it is an open question whether such models, which take into account two coupled heat diffusion equations (for ion and electron) with nonlinear thresholds and couplings, can be applied to the thermally decoupled electron-ion regime where the nonlocal  $T_e$  rise is mainly observed or not. In order to establish a convincing theoretical reconstruction of the core  $T_e$  rise due to the nonlocal effect, a further experimental investigation in extensive parametric space into the cause and effect of the nonlocal  $T_e$  rise is required. In this regard, further experimental study on helical systems is expected to contribute significantly, since helical systems have a quite different magnetic configuration (normally negative magnetic shear) and do not show a tokamak-like stiffness in the electron temperature profile.<sup>17</sup> This letter presents the characteristics of nonlocal  $T_e$  rise invoked by the edge cooling, which is observed for the first time in a helical plasma.

The experiments are carried out in the Large Helical Device (LHD), which has a heliotron-type magnetic configuration, with a magnetic axis position of  $R_{ax}=3.5$  m, an average minor radius of  $a=0.6$  m, and a magnetic field at the axis of 2.829 T.<sup>18</sup> The plasmas were started up and sustained by neutral beam injection (NBI) and overlapped with ECH, if not otherwise specified. The ECH beams (the applied frequencies: 82.7, 84, and 168 GHz) are focused near the  $R_{ax}$ .<sup>19</sup> The power of the neutral beam mainly goes into the electrons due to the high acceleration energy (for these experiments,  $\sim 140$  keV). Thus the electron loss channel dominates the ion loss channel. The temporal behaviors of  $T_e$  at different radii are measured with a 32-channel electron cyclotron emission (ECE) heterodyne radiometer with high time

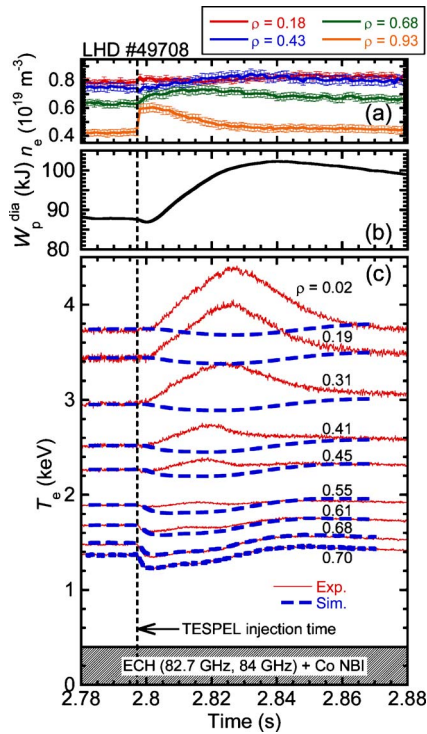


FIG. 1. (Color online). Temporal evolutions of (a) the electron density  $n_e$  measured with the FIR, (b) the diamagnetically measured plasma stored energy  $W_p^{\text{dia}}$ , and (c) electron temperature measured (solid line) with the ECE radiometer at different normalized minor radii. In (a) the local electron density is evaluated with the Abel inversion technique. The error bar with that is obtained by taking into account the positional error of the FIR chord, which is assumed to be within 5 mm. In (c) the simulated (broken line) temperature is also plotted. The TESPEL injection time is indicated as the vertical dashed line. Within the time displayed in the plots, the plasma is heated continuously by the ECH (injected power  $\sim 1.7$  MW) of 82.7 and 84 GHz and the co-injected NBI (injected power  $\sim 2$  MW).

resolution.<sup>20</sup> The  $T_e$  measured with the ECE radiometer is in good agreement with that with yttrium aluminum garnet (YAG) Thomson scattering system<sup>21</sup> in these experiments. In order to cool the edge region of the LHD plasma, a tracer-encapsulated solid pellet<sup>22,23</sup> (TESPEL) is injected into the LHD plasma from the outboard side of LHD. TESPEL consists of polystyrene  $[-\text{CH}(\text{C}_6\text{H}_5)\text{CH}_2-]$  as an outer shell, the diameter of which ranges around from 400 to 900  $\mu\text{m}$ , and tracer particles as an inner core. In these experiments, no tracer impurity is loaded into the TESPEL to reduce the possibility of improving the heating efficiency by the NBI attributed to the increased effective ionic charge.<sup>24</sup> The TESPEL penetrated into the LHD plasma ablates typically within  $\sim 1$  ms and provides a small amount of cold ions and electrons. They decrease the electron temperature at the periphery of the LHD plasma and then the negative temperature perturbation propagates toward the core plasma with a certain delay (cold pulse propagation).

Figure 1 shows the typical temporal evolutions of the electron density  $n_e$  measured with the far-infrared interferometer (FIR),<sup>25</sup> the diamagnetically measured plasma stored energy  $W_p^{\text{dia}}$  and the electron temperature measured with the ECE radiometer at different normalized minor radii for the plasma with the TESPEL injection. In this instance, the TESPEL is deposited outside  $\rho \sim 0.8$ . A significant rise of the

core  $T_e$  in response to the rapid edge cooling can be immediately seen in Fig. 1(c). The global energy confinement time can be increased by  $\sim 6\%$  due to the increase in the line-averaged electron density  $\bar{n}_e$  by  $\sim 11\%$  according to the energy confinement scaling from the international stellarator database.<sup>26</sup> As seen in Fig. 1, however, the quite different temporal behaviors among the  $n_e$ , the  $T_e$ , and the  $W_p^{\text{dia}}$  indicate that the improvement of the confinement based on the scaling has nothing to do with the core  $T_e$  rise observed. During the core  $T_e$  rising phase, no significant change in low- $m$  magnetohydrodynamics modes is observed and no density peaking occurs. The degradation of the increased  $T_e$  seems to propagate from the edge to the core. The time-dependent simulation result is also shown in Fig. 1(c). In this simulation, the perturbed heat transport equation based on a simple diffusion model is solved numerically (see Ref. 27 for details). The heat diffusivity used in the simulation, which has a radial dependence, is obtained by power balance analysis. The discrepancy between the experimental data and the simulated one is perceivable inside ( $\rho < 0.61$ ) of the plasma. Meanwhile, the  $T_e$  behavior on the outside ( $\rho > 0.61$ ) of the plasma shows a good agreement with the simulation result, that is, shows a cold pulse propagation induced by the local diffusive process. To measure whether the electron heat transport is improved or not when the core  $T_e$  rises due to the edge cooling, a transient analysis is carried out with a simple diffusion model but with the electron heat diffusivity  $\chi_e$  changing with time. In this model, the incremental electron heat flux  $\delta q_e$  can be written as<sup>1</sup>

$$\delta q_e = -n_e \chi_e \nabla \delta T_e - n_e \delta \chi_e \nabla T_e, \quad (1)$$

where  $n_e$ ,  $\nabla T_e$ , and  $\chi_e = -q_e / (n_e \nabla T_e)$  are the steady-state values just before the edge cooling, and  $\nabla \delta T_e$  and  $\delta \chi_e$  are the gradient of the perturbed  $T_e$  and the perturbed  $\chi_e$ , respectively. If  $\chi_e$  does not depend on  $\nabla T_e$ ,  $\delta \chi_e$  can be deduced from the behavior of the data points in the space of  $\delta q_e$  normalized by  $n_e$  vs  $\nabla \delta T_e$ . From the recent LHD experiment, no dependence or a very weak dependence of  $\chi_e$  on  $\nabla T_e$  has been obtained for the LHD plasmas.<sup>28</sup> Here, the  $\delta q_e$  can be evaluated by deforming the energy conservation equation for the electron perturbation,<sup>1</sup>

$$\delta q_e(r, t) = -\frac{1}{r} \int_0^r \frac{3}{2} n_e \frac{\partial \delta T_e}{\partial t} r' dr'. \quad (2)$$

In arriving at the above equation, the terms related to the perturbation of  $n_e$  and the perturbed source terms of the heat and particles are ignored in the energy conservation equation. Indeed, as the results of the experiment show,  $n_e$  in the region of interest almost remains the same just before and after the TESPEL injection considering the accuracy of the Abel inversion technique as seen in Fig. 1(a). Since the beam slowing-down time of the LHD NBI is very long at low density (e.g.,  $\sim 50$  ms at the value of  $n_e$ ,  $0.7 \times 10^{19} \text{ m}^{-3}$ ),<sup>30</sup> the impact of TESPEL injection on the NBI deposition profile just after the injection is almost negligible. The improvement of the ECH absorbed power due to the TESPEL injection is also negligible, since the ECH absorbed power just after the TESPEL injection is increased only by 0.05% com-

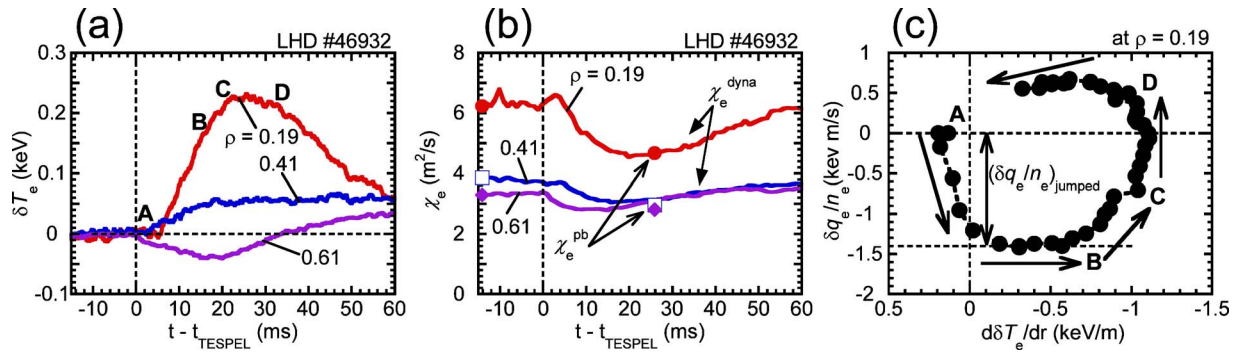


FIG. 2. (Color online). (a) Temporal evolution of the incremental electron temperature at three different minor radii around the TESPEL injection time  $t - t_{\text{TESPEL}}$ . (b) Temporal evolution of the dynamic electron thermal diffusivity  $\chi_e^{\text{dyna}}$ , which is estimated from both power balance analysis and transient analysis, at three different minor radii. The  $\chi_e^{\text{pb}}$ , which is evaluated only by power balance analysis, is plotted with symbols. (c) The incremental electron heat flux normalized by the electron density as a function of the gradient of the incremental electron temperature at  $\rho=0.19$  after the TESPEL injection. Each data point is obtained with an interval of 1 ms.

pared to that before the injection. Nevertheless, the transient analysis in the outer region ( $\rho > 0.7$ ) cannot be made due to the unignorable variation of the perturbed source of heat and particles. Figure 2(a) shows the response of the incremental electron temperature  $\delta T_e$  to the edge cooling in the LHD plasma, which is analyzed by the above transient analysis technique. As shown in Fig. 2(b), the dynamic electron thermal diffusivity  $\chi_e^{\text{dyna}} = \chi_{e0}^{\text{pb}} + \delta\chi_e$  shows a clear reduction after the edge cooling in the region of interest. Here  $\chi_{e0}^{\text{pb}}$ , which is defined as  $-q_e / (n_e \nabla T_e)|_{t-t_{\text{TESPEL}}=-14 \text{ ms}}$ , is estimated by power balance analysis and  $\delta\chi_e$  is obtained by the above transient analysis. The  $\chi_e^{\text{dyna}}$  at  $t - t_{\text{TESPEL}} = 26 \text{ ms}$  is in good agreement with the  $\chi_e^{\text{pb}}$ . The reduction of  $\chi_e$  seems not to propagate from the edge to the core. In order to understand the dynamics of electron heat transport, the time trace of the plasma at  $\rho=0.19$  after the edge cooling in the space of  $\delta q_e / n_e$  vs  $d\delta T_e / dr$  is plotted as shown in Fig. 2(c). It must be noted that the  $\delta q_e / n_e$  after the edge cooling [time A, indicated in Figs. 2(a) and 2(c)] simply dropped, while  $d\delta T_e / dr$  almost remains the same. Moreover, the back transition of the decreased  $\delta q_e / n_e$  to the preinjection level (from time B to time D) occurs accompanied by the slight change of  $d\delta T_e / dr$ . Since the local parameters in the core plasma did not change due to the edge cooling, the reduction of  $\delta q_e$  does not depend on those. Thus the abrupt increase in the core  $T_e$  observed in response to the rapid edge cooling of the LHD plasma can be regarded as the so-called nonlocal  $T_e$  rise observed so far only in many tokamaks.

The experimental results so far regarding the nonlocal  $T_e$  rise on LHD have characteristics similar to those of tokamaks. Figure 3(a) shows the temporal derivative of the electron temperature  $dT_e / dt$  in the core plasma (at  $\rho=0.12$ ) as a function of the line-averaged electron density at two different times. All the data in the figure are obtained with  $R_{\text{ax}} = 3.5 \text{ m}$  and  $B_{\text{ax}} = 2.829 \text{ T}$ . Just after the TESPEL injection (at  $t - t_{\text{TESPEL}} = 1 \text{ ms}$ ), both positive and negative  $dT_e / dt$ , which just appeared in response to the TESPEL injection, are observed for  $\bar{n}_e < 2.0 \times 10^{19} \text{ m}^{-3}$ . These fast responses of  $dT_e / dt$  cannot be explained by diffusive nature, although its sign is negative, as seen in Fig. 1(c). When 8 ms have elapsed since the TESPEL injection, a clear dependence of

the  $dT_e / dt$  on the  $\bar{n}_e$  is perceivable for  $\bar{n}_e < 2.0 \times 10^{19} \text{ m}^{-3}$ . Above  $\bar{n}_e \sim 2.0 \times 10^{19} \text{ m}^{-3}$ , a significant positive  $dT_e / dt$ , that is, the increase of the core  $T_e$ , in response to the edge cooling is no longer observed. The inverse relationship between the nonlocal  $T_e$  rise and the electron density as indicated in Fig. 3(a) is also observed in tokamaks.<sup>9</sup> The empirical condition  $n_e(0) / T_e(0)^{1/2} \leq 0.035 \times 10^{19} \text{ m}^{-3} / \text{eV}^{1/2}$ , which has been obtained in Ohmic plasmas on the Tokamak Fusion Test Reactor (TFTR),<sup>8</sup> can predict the density threshold for the occurrence of nonlocal  $T_e$  rise obtained in NBI+ECH plasmas on LHD. In many tokamaks, there is a perceivable delay in the increase of the core  $T_e$  after the edge cooling.<sup>9,12</sup> Also in LHD, such a time delay is observed as shown in Fig. 3(b). In the case of LHD, the time delay of the onset of a nonlocal  $T_e$

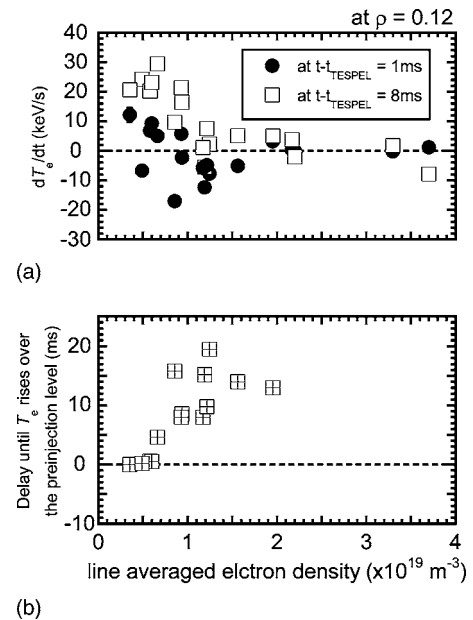


FIG. 3. (a) Temporal derivative of the electron temperature at  $\rho=0.12$  as a function of the line-averaged electron density of 1 ms after the TESPEL injection (closed circle) and 8 ms after that (open square). (b) The delay until the  $T_e$  rise over the level just before the TESPEL injection. The injected power of the NBI and overlapped ECH are approximately 2–3 and 1.2 MW, respectively.

rise seems to increase with the increase in  $n_e$ . The nonlocal  $T_e$  rise in the LHD plasmas is observed also when a small hydrogen pellet is injected as well as in tokamak plasmas. Thus the impurity seeding effect, such as radiative improved (RI) mode,<sup>31</sup> can be excluded as the main cause of the nonlocal  $T_e$  rise in LHD plasmas. The similarities in the nonlocal  $T_e$  rise between tokamaks and LHD may suggest that the sign of the magnetic shear does not play an important role in this phenomenon. It must be noted here that the comparison between LHD and Wendelstein 7-AS (W7-AS) stellarator, in which the nonlocal  $T_e$  rise has not been observed,<sup>14</sup> indicates that the magnetic shear itself and/or the existence of the rational values of the rotational transform at the plasma edge could be a crucial part of the nonlocal  $T_e$  rise. Further investigation on this matter will be performed on LHD. Although the physical mechanism of the nonlocal  $T_e$  rise still remains unclear, the similarities in the nonlocal  $T_e$  rise between tokamaks and LHD and the differences between LHD and W7-AS contribute to the investigation of the nonlocal transport phenomenon in toroidally confined plasmas.

The so far promising ITG-based models, which are being developed for the nonlocal  $T_e$  rise observed in tokamaks, suggest that the phenomenon is attributed to the suppression of ITG turbulence of which the ratio of  $T_e/T_i$  is the key parameter in the growth rate. Thus it is important to investigate the dependence of the phenomenon on the ratio of  $T_e/T_i$ , even though the applicability of the ITG-based transport models to the nonlocal effect observed in helical plasmas remains to be proved. (It is observed in helical devices that the ion transport degrades and the ion thermal diffusivity becomes higher than the electron thermal diffusivity accompanied by the increase of the  $T_e/T_i$  ratio,<sup>32,33</sup> which is consistent with the predictions of the ITG transport models.) Unfortunately, in the LHD, the plasma heating system based on the electron heating allows us to study the nonlocal  $T_e$  rise only under the condition of  $T_e/T_i > 1$ . The nonlocal  $T_e$  rise is observed also in NBI-only discharges. It should be noted here that the nonlocal  $T_e$  rise is also observed in plasmas sustained only by ECH ( $T_e/T_i > 1$  is understandably satisfied), which can completely rule out the contribution of the toroidal plasma current as a reason for the nonlocal  $T_e$  rise, even though it is mainly in Ohmic discharges that the nonlocal effect has been observed in many tokamaks. Since a low-energy positive NBI system is being developed now on LHD to provide strong ion heating, such a  $T_e/T_i$  dependence on the nonlocal effect will be studied shortly.

In conclusion, the core  $T_e$  rise in response to the rapid edge cooling induced by the TESPEL injection is observed for the first time in a toroidal helical plasma. This experimental result produces strong evidence that the core  $T_e$  rise as a manifestation of nonlocal transport phenomenon can take place in toroidally confined plasmas, not only in tokamak plasmas. The transport analysis shows that the clear reduction of the electron thermal diffusivity occurs when the core  $T_e$  is increased after the edge cooling. It shows also that the reversion of the electron thermal diffusivity to the preinjection level occurs. In the first stage of the reduction of the electron thermal diffusivity, there is a clear jump of  $\delta q_e$  al-

most without changing the  $\delta T_e$  gradient in the region of interest.

The authors acknowledge all of the technical staff of NIFS for their excellent support. They also would like to thank Professor O. Motojima (Director of NIFS) for his continuous encouragement. This work is supported by a Grant-in-Aid for Scientific Research from Japan Society for the Promotion of Science and a budgetary Grant-in-Aid No. NIFS05ULHH510 of the National Institute for Fusion Science.

- <sup>1</sup>N. J. L. Cardozo, *Plasma Phys. Controlled Fusion* **37**, 799 (1995).
- <sup>2</sup>J. D. Callen and M. W. Kissick, *Plasma Phys. Controlled Fusion* **39**, B173 (1997).
- <sup>3</sup>F. Ryter, C. Angioni, M. Beurskens *et al.*, *Plasma Phys. Controlled Fusion* **43**, A323 (2001).
- <sup>4</sup>U. Stroth, L. Giannone, H.-L. Hartfuss, the ECH Group, and the W7-AS Team, *Plasma Phys. Controlled Fusion* **38**, 611 (1996).
- <sup>5</sup>H. Yamada, K. Y. Watanabe, K. Yamazaki *et al.*, *Nucl. Fusion* **41**, 901 (2001).
- <sup>6</sup>S. Inagaki, K. Ida, N. Tamura *et al.*, *Plasma Phys. Controlled Fusion* **46**, A71 (2004).
- <sup>7</sup>S. V. Neudatchin, J. G. Cordey, D. Muir *et al.*, *Proceedings of the 20th EPS Conference on Controlled Fusion and Plasma Physics, Lisboa* (EPS, Geneva, 1993), Vol. I, p. 83.
- <sup>8</sup>M. W. Kissick, J. D. Callen, and E. D. Fredrickson, *Nucl. Fusion* **38**, 821 (1998).
- <sup>9</sup>P. Galli, G. Gorini, P. Mantica, G. M. D. Hogewij, J. de Kloe, N. J. Lopes Cardozo, and RTP team, *Nucl. Fusion* **39**, 1355 (1999).
- <sup>10</sup>X. L. Zou, A. Geraud, P. Gomez *et al.*, *Plasma Phys. Controlled Fusion* **42**, 1067 (2000).
- <sup>11</sup>G. M. D. Hogewij, P. Mantica, G. Gorini, J. de Kloe, N. J. Lopes Cardozo, and the RTP team, *Plasma Phys. Controlled Fusion* **42**, 1137 (2000).
- <sup>12</sup>F. Ryter, R. Neu, R. Dux *et al.*, *Nucl. Fusion* **40**, 1917 (2000).
- <sup>13</sup>K. W. Gentle, W. L. Rowan, R. V. Bravenec *et al.*, *Phys. Rev. Lett.* **74**, 3620 (1995).
- <sup>14</sup>H. Walter, U. Stroth, J. Bleuel *et al.*, *Plasma Phys. Controlled Fusion* **40**, 1661 (1998).
- <sup>15</sup>J. E. Kinsey, R. E. Waltz, and H. E. St. John, *Phys. Plasmas* **5**, 3974 (1998).
- <sup>16</sup>M. Kotschenreuther, W. Dorland, M. A. Beer, and G. W. Hammett, *Phys. Plasmas* **2**, 2381 (1995).
- <sup>17</sup>H. Yamada, S. Murakami, K. Yamazaki *et al.*, *Nucl. Fusion* **43**, 749 (2003).
- <sup>18</sup>O. Motojima, H. Yamada, A. Komori *et al.*, *Phys. Plasmas* **6**, 1843 (1999).
- <sup>19</sup>S. Kubo, T. Shimojuma, H. Idei *et al.*, *J. Plasma Fusion Res.* **78**, 99 (2002).
- <sup>20</sup>K. Kawahata, Y. Nagayama, S. Inagaki, Y. Ito, and LHD Experimental Group, *Rev. Sci. Instrum.* **74**, 1449 (2003).
- <sup>21</sup>K. Narihara, I. Yamada, H. Hayashi, and K. Yamauchi, *Rev. Sci. Instrum.* **72**, 1122 (2001).
- <sup>22</sup>S. Sudo, *J. Plasma Fusion Res.* **69**, 1349 (1993).
- <sup>23</sup>N. Tamura, S. Sudo, K. V. Khlopenkov *et al.*, *Plasma Phys. Controlled Fusion* **45**, 27 (2003).
- <sup>24</sup>Y. Takeiri, T. Shimojuma, S. Kubo *et al.*, *Phys. Plasmas* **10**, 1788 (2003).
- <sup>25</sup>K. Kawahata, K. Tanaka, Y. Ito, A. Ejiri, and S. Okajima, *Rev. Sci. Instrum.* **70**, 707 (1999).
- <sup>26</sup>U. Stroth, M. Murakami, R. A. Dory, H. Yamada, S. Okamura, F. Sano, and T. Obiki, *Nucl. Fusion* **36**, 1063 (1996).
- <sup>27</sup>S. Inagaki, T. Tamura, K. Ida *et al.*, *Phys. Rev. Lett.* **92**, 055002 (2004).
- <sup>28</sup>S. Inagaki, H. Takenaga, K. Ida *et al.*, *Nucl. Fusion* (submitted).
- <sup>29</sup>K. Tanaka, C. Micheal, A. Sanin *et al.*, *Nucl. Fusion* (to be published).
- <sup>30</sup>S. Morita, M. Goto, Y. Takeiri *et al.*, *Nucl. Fusion* **43**, 899 (2003).
- <sup>31</sup>A. M. Messiaen, J. Ongena, U. Samm *et al.*, *Phys. Rev. Lett.* **77**, 2487 (1996).
- <sup>32</sup>K. Ida, K. Kondo, K. Nagasaki *et al.*, *Plasma Phys. Controlled Fusion* **40**, 793 (1998).
- <sup>33</sup>K. Ida, T. Fujita, T. Fukuda *et al.*, *Plasma Phys. Controlled Fusion* **46**, A45 (2004).